Curr Microbiol (2011) 62:715–726
DOI 10.1007/s00284-010-9770-7

Nature-inspired Novel Drug Design Paradigm Using Nanosilver: Efficacy on Multi-Drug-Resistant Clinical Isolates of Tuberculosis

Dipankar Seth · Samrat Roy Choudhury · Saheli Pradhan · Siddhartha Gupta · Debjani Palit · Sumistha Das · Nitai Debnath · Arunava Goswami

Received: 17 July 2010 / Accepted: 8 September 2010 / Published online: 10 October 2010

Abstract Despite discovery of the pathogen more than 100 years ago, tuberculosis (TB) continues to be a major killer disease worldwide. Currently a third of world population is infected and multiple-drug-resistant (*mdr*) TB registers maximum mortality by a single pathogen. Nanomedicine provides enormous opportunity for developing novel drugs. We have recently demonstrated surface-modified-lipophilic-nanosilica as drug to combat malaria and 100% lethal virus, BmNPV. Nanosilver possesses inherent antibacterial properties, but toxicity is a major concern. We hypothesized that capping with nature-inspired biomolecules, bovine serum albumin (BSA) and Poly-n-vinyl-pyrrolidone (PVP) used as blood volume extender, might insure biosafety. BSA-nano-Ag was found to be more stable than PVP-nano-Ag at physiological pH. In this first ever study on clinical isolates collected from TB endemic areas, we report, BSA-nano-Ag act as potent anti-TB drug. Further study with (human serum albumin)-nano-Ag and core–shell-nano-Ag could increase the biocompatibility of oral TB drug formulations without compromising on the efficacy of the drug.

D. Seth · S. R. Choudhury (✉) · S. Pradhan · S. Das · N. Debnath · A. Goswami
Biological Sciences Division, Indian Statistical Institute, 203 B. T. Road, Calcutta 700108, West Bengal, India
e-mail: samratroychoudhury@gmail.com

D. Seth
e-mail: dipankarvet@yahoo.co.in

S. Pradhan
e-mail: saheli.pradhan@gmail.com

S. Das
e-mail: Sumistha.das@gmail.com

N. Debnath
e-mail: kholachithi@rediffmail.com

A. Goswami
e-mail: srabanisopanarunava@gmail.com; agoswami@isical.ac.in

S. Gupta
Department of Biochemistry, Biochemistry Research Wing, Institute of Postgraduate Medical Education & Research, 244 A. J. C. Bose Road, Calcutta 700020, West Bengal, India

D. Palit
Pathowynd Clinical Laboratory Inc, 29A Balaram Ghose Street, Calcutta 700004, West Bengal, India

Introduction

Nanomedicine provides enormous opportunity for developing novel drugs. We have recently demonstrated that surface-modified-lipophilic-nanosilica could be effectively used to combat malaria [1–5] and 100% lethal virus, BmNPV [5, 6]. We have also reported novel mechanisms of action of these nanoparticles [7].

Adverse drug reactions (ADR) of commonly used anti-TB drugs, worldwide like Streptomycin, Rifampicin, Pyrazinamide, and INH ranges from intolerance to hepatitis, neuropathy, optic nerve atrophy, etc. They require regular monitoring like liver function tests. Search for safer drugs propelled this study. Nanoscience derived tools like surface capping with natural biomolecule like Bovine Serum Albumin (BSA) and biocompatible chemical like Poly Vinyl Pyrrolidine (PVP) were considered to be valid options. It was anticipated that saturated surface capping would be able to mask the pure nano-Ag surface and thus would reduce toxicity without hampering efficacy. Before, the efficacy of the putative oral drugs is explored, stability at different pH is considered to be the most important parameter for oral administration as the molecule would

experience large variation in pH starting from esophagus to large intestine and other target tissues in the body. Moreover, body uptake of drugs is also dependent upon pH. This study, therefore, first observed the stability of the BSA- and PVP-capped nano-Ag at different pH and then explored the potential of these putative drugs toward growth inhibition of control TB strains (*Mycobacterium tuberculosis*) as well as strains isolated from clinical specimens like sputum or body fluids from one of the largest TB endemic epicenters of India. The effectiveness of BSA-capped nano-Ag and its mechanism of action against the *mdr* strains of *M. tuberculosis* (identified on the basis of conventional drug sensitivity testing) has been included in this study. Encouragingly, the results indicate that this novel design could be further extended for developing improved medicinal agents for combating multi-drug-resistant TB.

Materials and Methods

All experimental studies with TB unless otherwise mentioned were outsourced and performed at the biosafety facilities in the Pathowynd Clinical Laboratory Inc., Kolkata, India, which follows current laws and protocols for biosafety in India.

Preparation of Aqueous Solution of Nano-Ag

Nano-Ag directly conjugated to natural BSA protein molecules were produced as per standard protocol [8]. Silver nitrate ($AgNO_3$), sodium borohydride ($NaBH_4$, 95%), and 200 proof spectrophotometric-grade ethanol were purchased from Fisher (99.9%, HPLC grade). Bovine serum albumin (BSA, M.W 66,000) was purchased from Calbiochem and used without further treatment. Briefly, sodium borohydride (0.0023 g in 1 ml of water) was added to an aqueous solution of silver nitrate (0.0162 g) and BSA (0.0356 g) under vigorous stirring of 1000 rpm by a magnetic stirrer. The molar ratio of Ag^+: BSA was 28:1, and the molar ratio of Ag^+:$BH4^-$ was 1:1. The reaction volume was 40 ml, and contained 13.50 μmol BSA. The reaction was allowed to proceed for 1 h, and the product was purified by precipitation at −5°C, followed by cold ethanol filtration. Nanopure water (18.2 m≏) from Sartorius was used throughout the experiment. Poly-n-vinyl-pyrrolidone (PVP, Mw = 40,000) purchased form Aldrich was used to prepare PVP-capped nano-Ag. The silver sol was prepared by reduction of Ag + ions in presence of ethanolic solution of PVP. The weight ratios of metal salt to PVP were 1:5, 1:10, and 1:20. The solution was kept under vigorous stirring and a clear yellow solution was obtained. The reduction was carried out at 70°C in a thermostatic water bath with reflux unit for 30 min [9].

Characterization of BSA- and PVP-Capped Nano-Ag

BSA- and PVP-capped nano-Ag particles were subjected to UV–VIS, DLS, TEM, and SEM analyses. 60 μl of silver nanoparticles was mixed in 3 ml of nanopure water (Arium 61316 and 611VF, Sartorius Inc., USA). UV–Visible absorption spectra (Perkin-Elmer Inc., USA; model: double beam lambda 25) were recorded with a 1-cm quartz cell. DLS (Malvern instruments, UK; model nano-S) analysis was done to study the size distribution of BSA- and PVP-capped nano-Ag. Further characterization was done by Transmission Electron Microscopy (TEM) (Joel Inc., USA; model JEM 2010). For transmission electron microscopy (TEM) studies, 15 μl of BSA- and PVP-capped nano-Ag particles were deposited on copper grids (Pro Sci Tech Inc., Australia; 300 mesh) under laminar hood and were allowed to air dry in a UV-sterilized condition and data were collected. During scanning electron microscopy (SEM) studies, *Mycobacterium* smears were prepared on 1 × 1 cm xylene cleaned glass slides and air dried followed by overnight glutaraldehyde fixation at 4°C. Each slide was coated with gold–palladium at 5 mA by SC7620 sputter-coater. The samples were analyzed by SEM-FEI QUANTA 200 (FEI Inc., USA). Stability of BSA- and PVP-capped nano-Ag in physiologically relevant salt solution (0.9% pure NaCl), temperature (37–80°C), and serum (Bovine serum, GE Healthcare) was monitored by UV–VIS for 1 h and time series data were generated. Similarly, structural stability of BSA- and PVP-capped nano-Ag with change in pH (fine probe pH meter; Sartorius; model PB 11) and temperature over 24 h time were recorded. Structural stability of BSA- and PVP-capped nano-Ag in salt, serum, different pH and temperature was studied by UV–VIS and DLS, as described above.

Clinical TB Samples

Sputum samples were collected from the pulmonary TB patients visiting state hospital outdoor clinics. Body fluids (pleural and peritoneal) are collected from extra-pulmonary TB patients visiting pathology department of State hospitals. All samples were collected maintaining proper sterility. Bioethical permissions from respective departments were obtained before collection of samples. Control strains like H37RVof *M. tuberculosis* and *M. xenopi* were obtained from the National Culture Collection of Tuberculosis Research Centre, India. Sputum samples were liquefied and decontaminated using equal volume of a mixture of 4% NaOH and N-acetyl-L-cysteine (NALC) for 30 min at room temperature. After decontamination, sample was neutralized by sterile PBS (pH 6.8) and centrifuged at 3600 *g* for 30 min.

Supernatant was discarded and loose pellet was resuspended in sterile distilled water [10]. The body fluids were concentrated by spinning down the whole fluid, discarding the supernatant and collecting the pellet maintaining sterility for further use [11]. Resuspended pellets of all specimens (sputum and body fluids) were stained by standard Ziehl-Neelson (Z-N) method for demonstration of Acid Fast Bacilli (AFB) [AFB Kit, Himedia Lab, India] and were examined for the presence of AFB with microscope (oil-immersion; Zeiss Axiolab, Germany). Smears recorded as positive in standard AFB scale and data per 100 fields were collected as per RNTCP (Revised National Tuberculosis Control Program, WHO) guidelines as described in Table 1 [12].

In Vitro Culture of *Mycobacterium tuberculosis*

Sterile clinical specimens, standard strains of H37 RV of *M. tuberculosis* and *M. xenopi* were grown both in Lowenstein-Jensen (L-J) slants (solid media) and Middlebrook 7H9 broth (liquid media) incubated for 5 weeks (solid media) and 3 weeks (liquid media) (Fig. 1). Cultures were grown at 35°C in dark within an atmosphere of 5% CO_2 and 70% humidity (RH). Standard colony and surface pellicle counting was done [13]. Figure 1a shows the typical Tb collection vials from the clinical specimens.

Biochemical Assays and PCR

Conventional biochemical assays, viz., nitrate reduction, catalase production, and niacin production were done for identification of different strains of *M. tuberculosis* as per kit protocols supplied by manufacturer (Himedia Lab, India) (Fig. 1) [14]. Genomic DNA was mini-prepped from aforesaid pelleted clinical specimens as well as control strains (colony and broth) using modified lysis method [13]. Multiplex PCR using three pairs of oligonucleotide primers representing 65 kd Hsp protein, Dnaj gene, and IS6110 with expected band sizes of 165, 365, and 541 bp, respectively, were performed (Himedia Lab, India) [15]. Control *M. tuberculosis* are expected to show amplification of all three targets, whereas atypical *Mycobacteria* like *M. xenopi* (MOTT organisms) would show amplification of one or two target sequences. Figure 1e, f shows results of multiplex PCR used for typing all TB samples.

Table 1 TB smears recorded as positive in standard AFB scale and data per 100 fields were collected as per RNTCP (Revised national tuberculosis control program, WHO) guidelines

No. of AFB	Interpretation
No AFB in 100 O.I.F	Nil
1–9/100 O.I.F	Scanty
10–99/O.I.F.	(+)
1–9/O.I.F	(++)
10–99/O.I.F	(+++)

Antimicrobial Properties of Nano-Silver

Three TB clinical specimens isolated from three different sites, i.e., from sputum, peritoneal, and pleural fluid, respectively, and two control strains of *M. tuberculosis* and *M. xenopi* were included in the study. Minimum inhibitory concentration (MIC) of BSA- and PVP-capped nano-Ag particles against clinical and control samples were determined. All strains were inoculated in two batches of 5 ml Middlebrook 7H9 broth. 1.6, 4, 8 μg/ml of nanoparticles were added immediately to the first batch. In the second batch, same graded concentrations of nanoparticles (1.6, 4, and 8 μg/ml) were added to the 20 days old broth culture to demonstrate the subsequent growth inhibition or lysis of bacteria by nanoparticles and were monitored for another 4 weeks. Bacterial growth was confirmed by appearance of turbidity in the media Z-N staining from centrifuged deposits and subsequent appearance of colonies on subculture on L-J slant. As already mentioned in order to quantify the amount of growth, RNTCP (Revised National Tuberculosis Control Program) guidelines were used for AFB smears [12]. Positive control experiments utilized bacterial inoculums without any nanoparticles and negative control contained only nanoparticles (8 μg/ml) without any bacterial inoculums.

Microarray Experiments

All microarray experiments were outsourced to Agilent Technologies Inc. and done in triplicate on Agilent platforms. Following nanoparticles were used for this experiment—BSA-capped nano-Ag, nano-silica, nano-aluminosilicate, nano-ZnO, nano-gold. Except BSA-capped nano-Ag, similar sized were custom made from M/S MKNANO Inc, Canada. One-color protocols were used where one labeled RNA sample was hybridized to each microarray. Agilent used its own method or software to generate a quantitative signal value and a qualitative detection call for each probe on the microarray. *Csdg* wild-type strain of *Drosophila melanogaster* were fed with nanoparticles 8 μg/ml with standard maize meal (added after

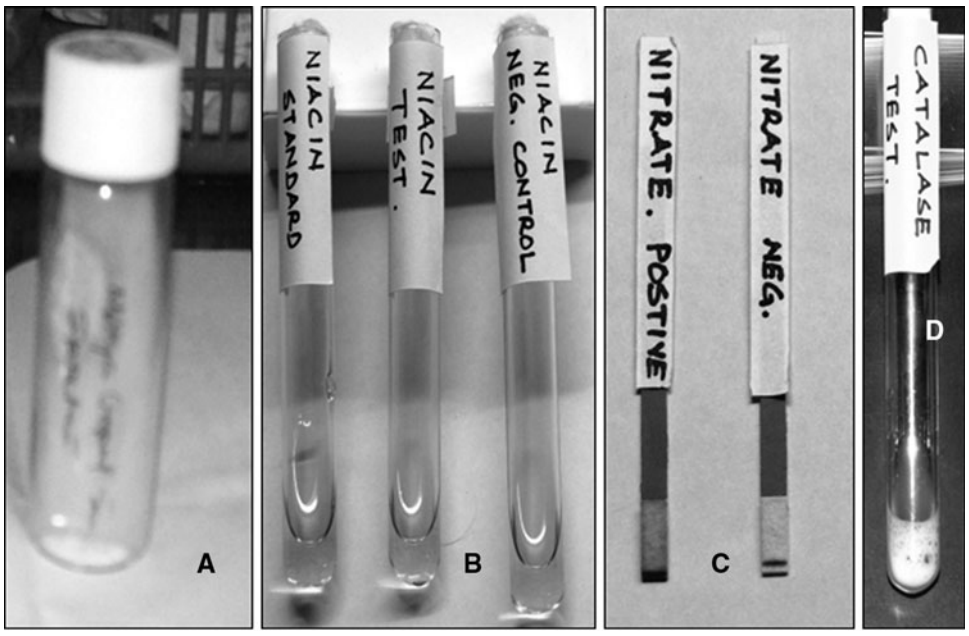

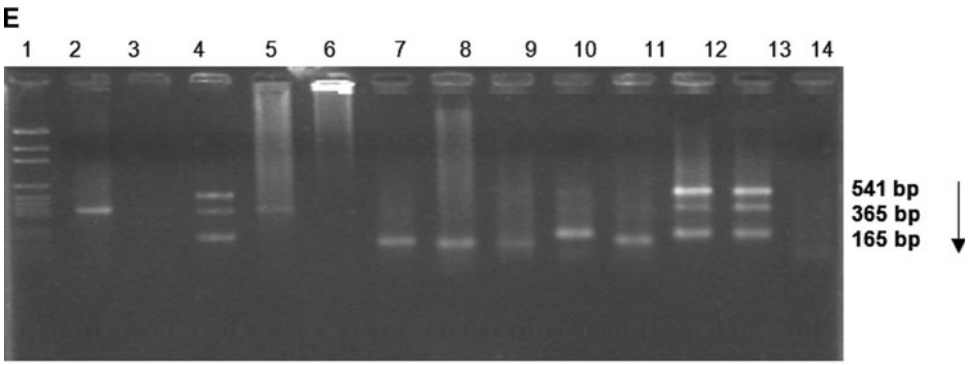

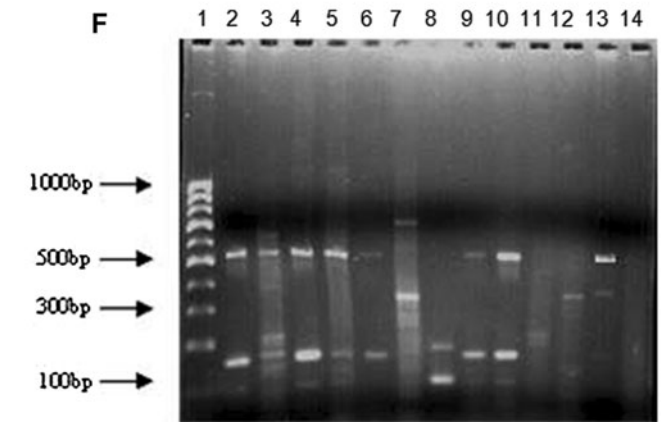

Fig. 1 **a** *Mycobacterium* culture, **b** Niacin test, **c** Nitrate test, **d** Catalase test. **e** Multiplex PCR amplification of 165, 365, and 451bp regions if the clinical specimens and control strains of *M. tuberculosis* and Non tubular mycobacteria (MOTT) on 2% agarose gel. *Lane 1* pGEM molecular marker, *lane 2–3* patients' sample (Pleural fluid), *lane 4* H37RV (control strain) of *M. tuberculosis*, *lane 5–6* patients' sample (Peritonial fluid), *lane 7–9* other Atypical mycobacteria, *lane 10–12* sputum sample of patients, *lane 13* positive control, *lane 14* negative control. **f** Multiplex PCR amplification of 165, 365, and 451 bp regions if the clinical specimens of *M. tuberculosis* and Non tubercular mycobacterium on 2.5% agarose gel. *Lane 1* 100 bp molecular marker, *lane 2–12* patient samples, *lane 13* positive control, *lane 14* negative control

autoclaving in sterile condition) for a period of 15 days, and RNA were prepared by Agilent Technologies. Before and after hybridization experiments, all quality control parameters were tested in triplicate by Agilent Technologies following the manufacturer's protocols.

Results and Discussion

Despite the discovery of the *M. tuberculosis* more than a hundred years ago, tuberculosis (TB) continues to be a major killer disease worldwide. Currently about a third of

the world population is infected with TB and related pathogens. It registers the highest mortality by a single pathogen [16] accounting for about 3 million deaths and about 10 million new cases each year. This corresponds to more than 7000 deaths per day and 1000 new cases per hour each day [17]. In India each year, about 2 million patients develop active disease and up to half a million die [18]. Moreover, emergence of multi-drug-resistant (*mdr*) strains and their sinister association with HIV/AIDS has posed a serious threat to the TB control program worldwide [19]. *mdr* is associated with high mortality rate of 50–80% and spans a relatively short time (4–16 weeks) from diagnosis to death [20]. Chemotherapy for TB was possible with the discovery of streptomycin in mid-1940s. The introduction of Rifampicin in the early 1970s heralded the era of effective short course treatment. Pyrazinamide and INH also contributed much to it. But, even today effective chemotherapy requires 6 to 18 months of treatment depending on the nature and site of the disease. Failure of remission by first line of drugs in 3–4 months requires introduction of a second line of drugs. Anti-tubercular drugs have serious Adverse Drug Reactions (ADR) including intolerance, hepatitis, neuropathy, optic nerve atrophy, etc. They should be used with extreme caution in pregnancy and lactation due to narrow margin of safety. Moreover, continuous monitoring of liver function test, neurological deficiencies, etc. is required. The total cost of the treatment is also high considering the relatively long span of treatment [21].

The anti-microbial property of colloidal silver is well known since long and a considerable amount of investigations has been carried out to establish its potential application in therapeutics [22]. But, little information is available as of date regarding its stability in different biological fluids, physiological salt solution, pH, and thermal stability. Colloidal silver is toxic and we hypothesized that surface capping with natural ligands like BSA might also reduce the toxicity. While considering nanosilver as a putative drug and controlled release thereof [23, 24], knowledge of stability is of paramount importance. Moreover, research efforts on the efficacy of the nanosilver on clinical specimens are scanty.

Characterization of BSA- and PVP-Capped Nano-Ag

It was previously demonstrated that a wide range of silver nanoparticles could be produced by varying the ratio of Ag and BSA/PVP. The size range of BSA-capped silver nanoparticle (BSA-Ag) was found to be 5–9 nm. On measuring TEM images of 100 particles, the average size was estimated to be 5.74 nm (Fig. 2).The inset picture in Fig 2 shows the characteristic diffraction pattern of BSA-capped nano-Ag. BSA-capped nano-Ag shows surface plasmon peak at 401.1 nm. BSA-capped nano-Ag particles were found to be stable at physiological salt solution like L-J media and Middle-brooks media, with a minor shift of the UV–VIS peak by 3 nm (Fig. 3). Stability studies were monitored for 24 h.

Silver nanoparticles were directly conjugated to BSA protein molecules in aqueous solution. Serum albumin is a

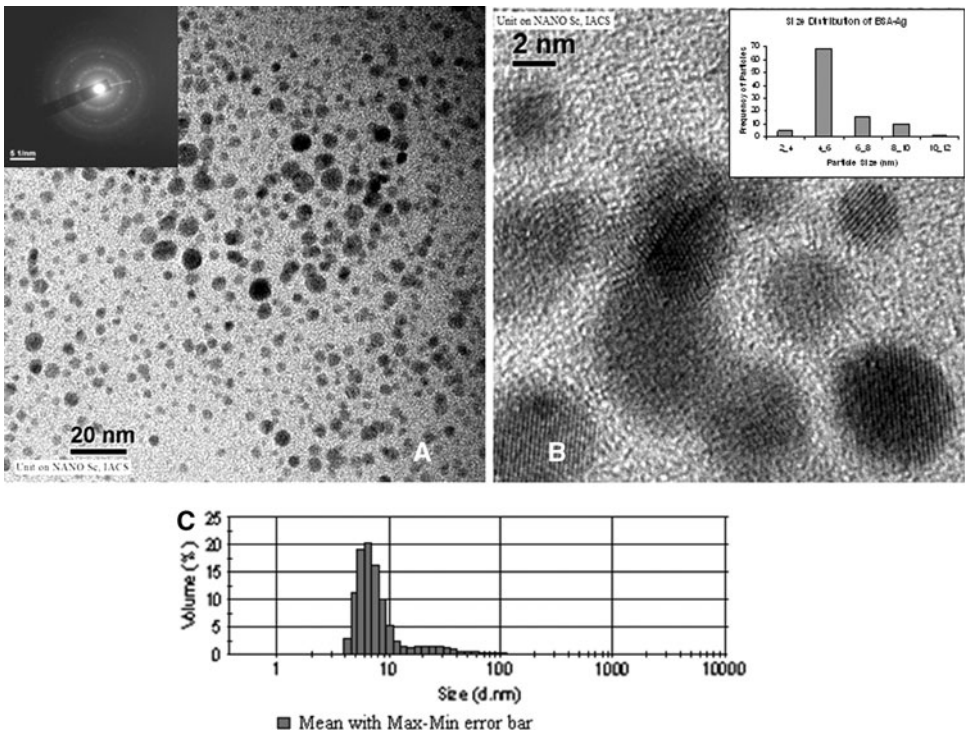

Fig. 2 **a** TEM pictures of BSA-Ag nanoparticles; *Inset* Diffraction pattern of PVP-Ag nanoparticles; **b** HR-Image; *Inset* Size distribution; **c** DLS size distribution

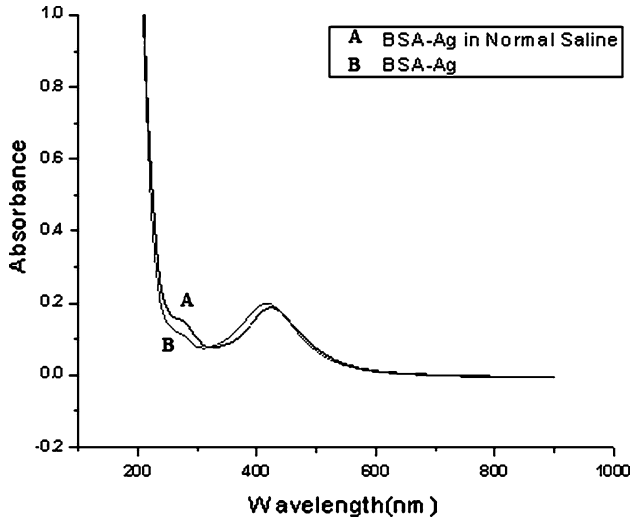

Fig. 3 Stability of BSA-capped Ag-nano in phsiological salt solution

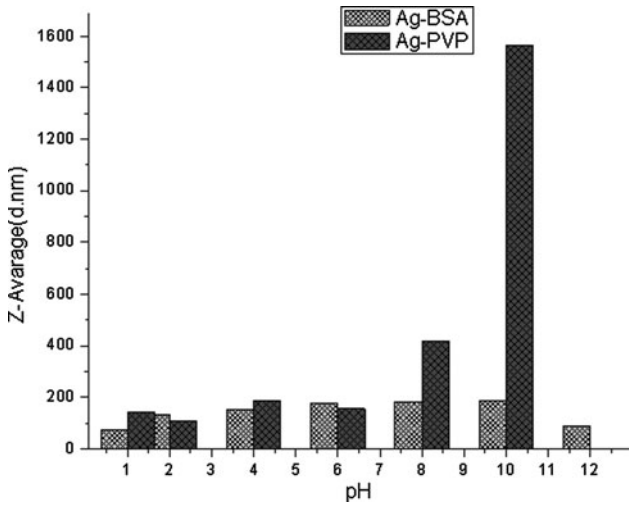

Fig. 5 pH stability studies of BSA-and PVP-capped nano-Ag. *Inset* shows that PVP-Ag in stblet at pH 2.0, but beyond pH 10.0 PVP is completely removed from the silver

globular protein, and is the most-abundant protein in blood plasma. Bovine serum albumin (BSA) is a single polypeptide chain composed of 583 amino acid residues. The strongest interactions of BSA with silver would likely involve 35 thiol-bearing cysteine residues [8]. This is probably due to the fact that Ag and S being highly polarisable atoms, a very stable soft acid (Ag)–soft base (S) interaction takes place in accordance with the HSAB (Hard Soft Acid Base) principle. It is noteworthy that Ag has been found to form stable compounds like $AgNO_3$, Ag_2S, etc. Using sodium borohydride, a strong reducing agent, BSA was stabilized on nano-Ag via direct bonding with these thiol bearing cysteine residues and this might have provided steric protection due to the bulkiness of the protein.

$$2AgNO_3 + 2NaBH_4 + 6H_2O + 2BSA\ [\text{capping agent}] = 2[Ag^0] - BSA(\text{capped Ag}) + 7H_2 + 2B(OH)_3 + 2NaNO_3$$

PVP is a linear polymer and stabilizes the nanoparticle surface via bonding with the pyrrolidone ring. Infrared (IR) and X-ray photoelectron spectroscopy (XPS) studies have revealed that both oxygen and nitrogen atoms of the pyrrolidone ring can promote the adsorption of PVP chains onto the surface of silver (data not shown).

PVP-capped silver nanoparticles (PVP nano-Ag) show a size distribution of 6–45 nm with an average size of 28.33 nm (Fig. 4). PVP-capped nano-Ag shows typical surface plasmon peak at 423 nm. PVP-capped nano-Ag begins to destabilize pH 7.0 onward in L-J media and Middle-brooks media (Fig. 5). PVP-capped nano-Ag were found to be more stable at elevated temperatures (>60°C) (data not shown). BSA-capped and PVP-capped nano-Ag particles were found to be equally stable in the physiological body temperature range. Salt (0.9% pure NaCl) and serum (20% solution of commercially available serum) did

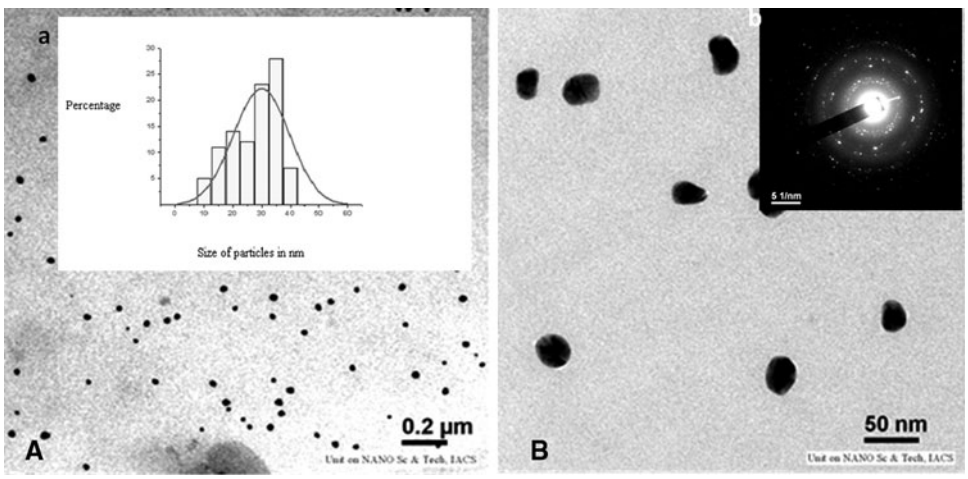

Fig. 4 TEM pictures of PVP-capped nano-Ag particles, **a** low resolution (*Inset* DLS size distribution); **b** high resolution (*Inset* Diffraction pattern)

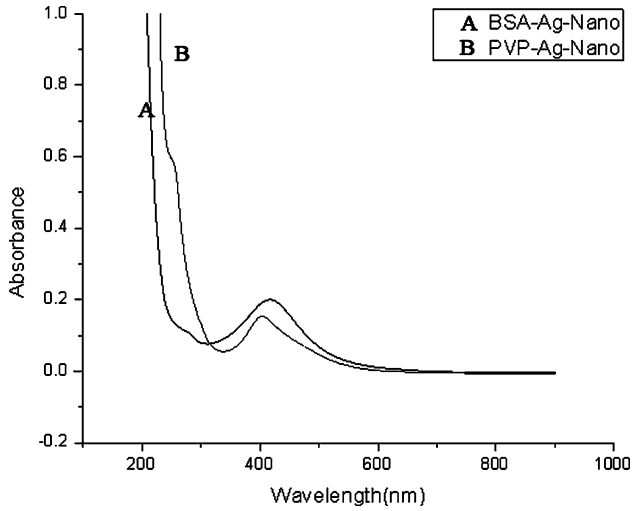

Fig. 6 Plasma peak of BSA- and PVP-capped silver nano-Ag at 401.1 and 423 nm, respectively

not induce aggregation of both BSA- and PVP-capped nano-Ag particles (Fig. 6).

Therefore, based on the aforesaid stability studies BSA-capped nano-Ag were used for further anti-mycobacterium efficacy studies in vitro (data not shown) and in vivo.

Inhibitory Assay of BSA-Ag on *M. tuberculosis*

Five different strains of *Mycobacterium* have been used in this study, of which four are of *M. tuberculosis* (one is a control strain, i.e., H37RV and three others are clinical isolates from sputum and body fluids of TB patients). The fifth strain is of *M. xenopi*, which is an atypical or MOTT (*Mycobacterium* other than TB) organism causing opportunistic infection in immunocompromised hosts [21]. All experiments were done with at least 5–6 replications unless otherwise specifically mentioned. In the first set of each batch, the bacterial inoculums were added in three tubes containing Middlebrook's broth and increasing concentration of nanosilver particles (8, 20, and 40 μg in 5 ml broth). A positive control set by a pure broth is culture of a Mycobacterial strain without any nanoparticle, whereas the negative control contained only 100 μg of nanosilver particles without any inoculums. In the second set, 1.6, 4, 8 μg/ml broth, BSA-capped nano-Ag were added in 20 days old broth culture (judged by O. D. value at 650 nm, appearance of turbidity, AFB tests) and lytic effect of the nanosilver particles were studied 20 day old established cultures (Table 2). *M. xenopi* shows complete growth inhibition in all the concentrations of nanosilver. No strain of *M. tuberculosis* showed any growth inhibition at concentrations of 1.6 μg/ml (8 μg/ml). At 4 μg/ml concentration, growth is partially inhibited in different strains of *M. tuberculosis* whereas in (8 μg/ml) complete growth inhibition occurred for all four strains (Table 3). In the next batch, effect of nanosilver particles is observed after 20 days of addition of nanoparticles. At 1.6 μg/ml concentration, there was almost no lysis except in *M. xenopi* (showing a scanty growth even in the positive control) At 4 μg/ml concentration, lysis was observed in the first two tubes (isolates from clinical specimens) but not in the culture containing isolates from the pleural fluid and

Table 2 Growth data when BSA-capped nano-Ag was added in 20 days old TB culture

Strain	Positive control	Nano-Ag 1.6 μg/ml	Nano-Ag 4 μg/ml	Nano-Ag 8 μg/ml	Negative control
M. tuberculosis from sputum	(++)	(++)	No growth	No growth	No growth
M. tuberculosis from peritoneal fluid	Scanty	Scanty	No growth	No growth	No growth
M. tuberculosis from pleural fluid	(+)	(+)	(+)	No growth	No growth
M. tuberculosis H37RV	(++)	(++)	(+)	Scanty	No growth
M. xenopi	Scanty	No growth	No growth	No growth	No growth

Table 3 Growth data when inoculums and nanosilver were added simultaneously

Strain	Positive control	Nano-Ag 1.6 μg/ml	Nano-Ag 4 μg/ml	Nano-Ag 8 μg/ml	Negative control
M. tuberculosis from sputum	(++)	(+)	No growth	No growth	No growth
M. tuberculosis from peritoneal fluid	Scanty	Scanty	No growth	No growth	No growth
M. tuberculosis from pleural fluid	(+)	(+)	Scanty	No growth	No growth
M. tuberculosis H37RV	(++)	(++)	(+)	No growth	No growth
M. xenopi	Scanty	No growth	No growth	No growth	No growth

Table 4 Comparative study of sensitivity of Mycobacteria to conventional anti-tubercular drugs and different concentrations of BSA-capped nano-Ag

Strains	Rifampicin (2 μg/ml)	INH (5 μg/ml)	Nano-Ag 1.6 μg/ml	Nano-Ag 4 μg/ml	Nano-Ag 8 μg/ml
M. tuberculosis from sputum	Sensitive	Resistant	Resistant	Sensitive	Sensitive
M. tuberculosis from peritoneal fluid	Sensitive	Sensitive	Resistant	Sensitive	Sensitive
M. tuberculosis from pleural fluid	Resistant	Resistant	Resistant	Partially sensitive	Sensitive
M. tuberculosis H37RV	Sensitive	Sensitive	Resistant	Partially sensitive	Sensitive
M. xenopi	Sensitive	Sensitive	Sensitive	Sensitive	Sensitive

the control strain. At the highest concentration, complete lysis was observed in all plates (Table 3). A comparative study of growth inhibition by BSA-capped nano-silver particles along with standard anti tubercular drugs (Rifampicin and INH) are compiled in Table 4. The strain isolated from the pleural fluid showed in vivo resistance to both Rifampicin (2 μg/ml) and INH (5 μg/ml) and by definition of pharmacology, it can be marked as a Multi Drug Resistant (*mdr*) strain. But even this strain is sensitive to 8 μg/ml concentration of BSA-capped nano-Ag.

In order to decipher the mechanism of action of silver nanoparticles, UV–VIS, SEM, and TEM studies were performed. BSA-capped nano-Ag alone shows peak at 401.1 nm and *Mycobacterium* alone gives a peak at 580 nm. We hypothesize that *Mycobacterium* and control BSA-capped nano-Ag particles conjugation complex gives the intermediate peak at 421 nm (Fig. 7). High resolution (HR) SEM studies revealed that BSA-capped nano-Ag wrinkles the cell surface and affects the integrity of the surface of the bacterial cell wall (Fig. 8). Eventually, the cytoplasmic material is extruded from the cell leading to the collapse of the cell. The collapsed cell then coalesces to form an amorphous mass of cell debris (data not shown). Figure 9a shows the high resolution TEM images of the surface of control *Mycobacterium* and Fig. 9b shows the data on the interaction of the BSA-capped nano-Ag and the bacteria. The inset in Fig. 9a shows turbidity clearly indicating the growth of TB bacteria whereas the inset in Fig. 9b is control. Further, low and HR-TEM studies revealed that BSA-capped nano-Ag particles enter inside the *Mycobacterium* cell (Fig. 10a , b) and were found to form precipitates as indicated by arrows (Fig. 10c, d). Therefore, BSA-capped nano-Ag kills *Mycobacterium* in a completely different fashion from that of antibiotics commonly used for treating TB. We may conclude that these nanaoparticles damage the cell wall and also on gaining entry into the cell tend to disrupt physiological processes via pathways ill understood at present. The combination of both these effects might be the reason for the startling observation that *mdr* strains fail to survive at higher dose of nanosilver. At present, we are investigating the cellular mechanisms.

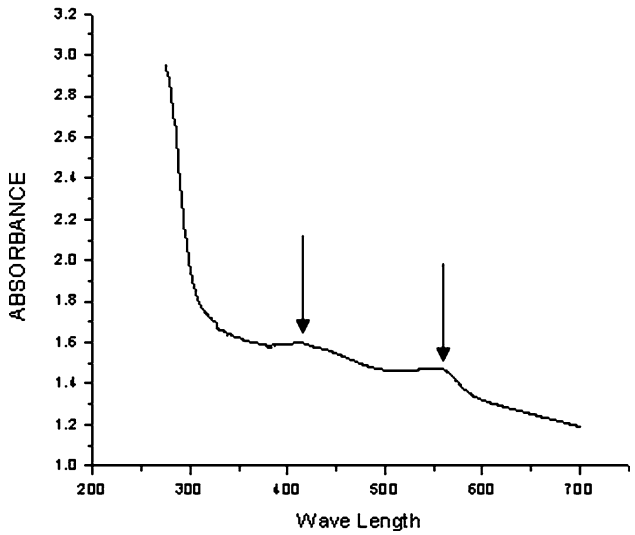

Fig. 7 UV–VIS spectrum showing interaction between *mycobacterium* and BSA-capped nano-Ag

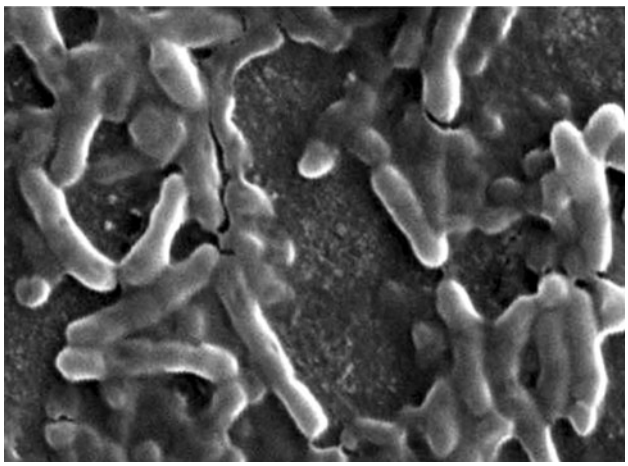

Fig. 8 High resolution SEM images showing BSA-capped nano-Ag treated destabilizes TB cell membrane

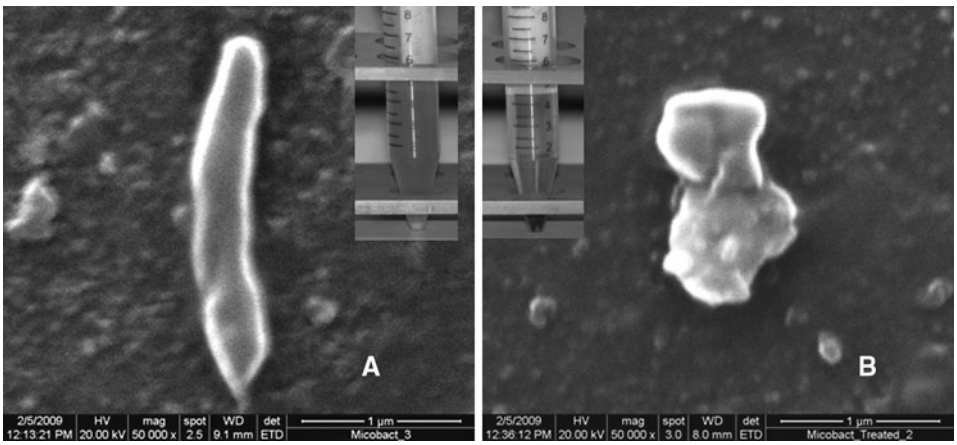

Fig. 9 **a** Control TB (*Inset* turbid liquid culture of TB showing growth); **b** TB treated with BSA-capped nano-Ag (*Inset* clear culture showing no growth)

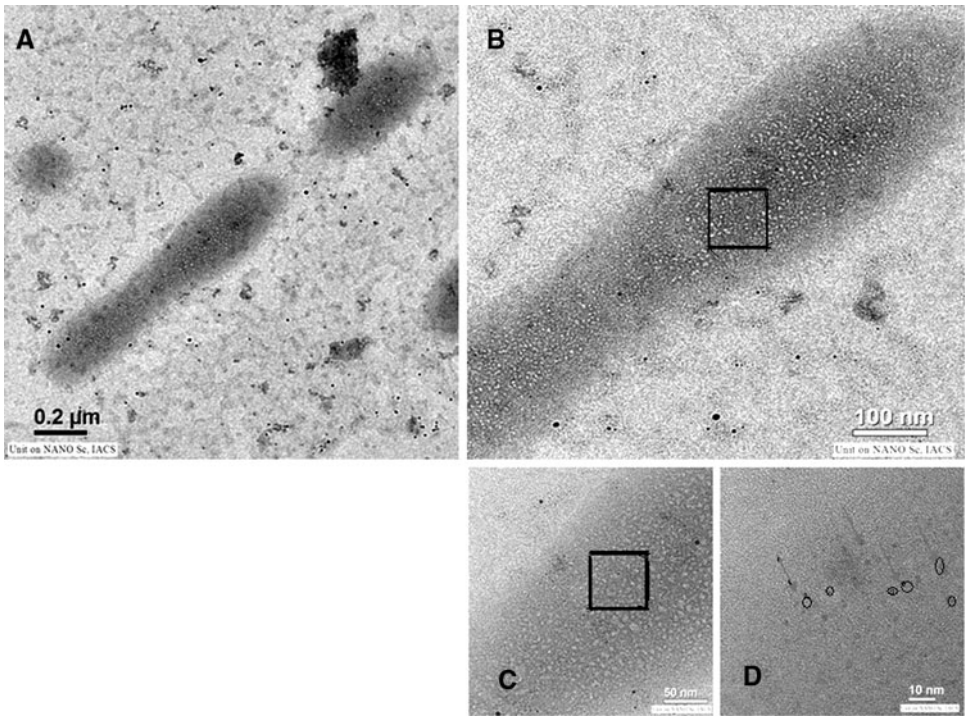

Fig. 10 **a** Low resolution TEM images of the BSA-capped nano-Ag attached to bacteria; **b**, **c**, and **d** Higher resolution images of **a**. *Insets* and *Arrows* in **c** and **d,** respectively, mark the entry of the nano-Ag particles inside the bacterial cell

Table 5 Comparative studies on the changes in level of expression of *Drosophila melanogaster* gustatory receptor genes when fed with BSA-capped nano-Ag and other nanoparticles

Agilent code	Control	Nano-SiO2	Nano-Al-SiO2	Nano-Au	Nano-Ag	Nano-ZnO	Protein name	Ligands
GT_09_P064191	0.91	0.88	1.33	1.15	3.05	1.23	Gustatory receptor 57a	
GT_09_P056871	0.81	2.16	1.16	2.26	0.80	0.67	Gustatory receptor 64c	
GT_09_P068516	0.81	4.25	1.12	4.29	1.28	0.22	Gustatory receptor 8a	
GT_09_P015086	0.77	0.84	0.99	1.31	1.07	1.65	Gustatory receptor 64f	
GT_09_P057131	0.98	0.86	0.98	0.87	2.14	0.95	Trapped in endoderm-1 (Gr)	
GT_09_P029251	0.90	2.22	0.86	3.10	0.54	0.89	Gustatory receptor 64d	
GT_09_P056911	1.12	5.22	0.86	1.90	2.49	2.25	Gustatory receptor 28b	
GT_09_P075876	1.11	1.03	0.82	1.08	0.86	4.24	Gustatory receptor Gr89a	Sugar
GT_09_P064206	0.86	0.82	0.75	0.84	0.51	1.02	Gustatory receptor 43a	
GT_09_P056956	0.99	1.56	0.70	2.47	1.03	1.66	Gustatory receptor 10a	

Table 5 continued

Agilent code	Control	Nano-SiO2	Nano-Al-SiO2	Nano-Au	Nano-Ag	Nano-ZnO	Protein name	Ligands
GT_09_P064256	1.06	0.86	0.64	1.01	1.60	1.20	Gustatory receptor 22f	
GT_09_P037691	1.28	2.58	0.62	4.24	3.30	0.54	Gustatory receptor 10b	
GT_09_P056906	1.16	2.30	0.62	2.03	3.33	1.10	Gustatory receptor 36a	
GT_09_P028126	0.91	1.10	0.62	1.54	0.80	0.46	Gustatory receptor 61a	
GT_09_P056886	1.18	3.11	0.62	5.53	3.21	0.55	Gustatory receptor 59b	
GT_09_P064186	1.13	1.85	0.61	2.05	3.18	0.56	Gustatory receptor 58a	
GT_09_P171580	1.12	4.26	0.61	5.25	3.29	0.55	Gustatory receptor 22d	
GT_09_P064246	1.04	6.30	0.61	6.09	3.26	0.55	Gustatory receptor 23a	
GT_09_P056841	1.17	3.06	0.61	4.11	3.27	0.53	Gustatory receptor 93d	
GT_09_P064151	1.18	1.18	0.58	1.99	2.98	1.14	Gustatory receptor Gr65a	
GT_09_P057236	1.37	4.48	0.58	7.42	2.99	0.54	Gustatory receptor Gr36d	
GT_09_P064211	1.25	4.38	0.57	3.77	3.26	1.22	Gustatory receptor 39a	
GT_09_P072351	0.89	1.27	0.57	1.59	0.33	0.27	Gustatory receptor 98a	
GT_09_P056951	1.31	3.70	0.56	2.00	3.13	0.60	Gustatory receptor 22a	
GT_09_P009811	1.12	2.52	0.55	1.93	3.22	0.55	Gustatory receptor, Trehalose-sensitivity	
GT_09_P064241	1.09	3.37	0.48	2.66	1.59	1.32	Gustatory receptor 28a	
GT_09_P064236	0.98	1.41	0.45	0.92	0.16	0.89	Gustatory receptor 32a	
GT_09_P064161	0.97	1.21	0.44	1.95	0.21	1.03	Gustatory receptor 59f	
GT_09_P056941	1.06	4.13	0.40	4.33	2.17	0.47	Gustatory receptor 22c	
GT_09_P064231	1.02	1.07	0.39	0.29	0.43	1.03	Gustatory receptor 39b	Bitter
GT_09_P064201	0.76	2.57	0.37	3.93	0.94	0.62	Gustatory receptor 47a	
GT_09_P053881	1.06	1.34	0.37	1.89	0.25	0.96	Gustatory receptor 66a	
GT_09_P064171	1.00	2.76	0.35	3.41	1.74	0.32	Gustatory receptor 59d	
GT_09_P056861	0.63	2.03	0.34	1.86	1.92	0.65	Gustatory receptor 85a	
GT_09_P064166	0.92	2.89	0.34	4.12	1.82	0.30	Gustatory receptor 59c	
GT_09_P056891	0.76	2.18	0.33	3.77	0.60	0.37	Gustatory receptor 59a	
GT_09_P056901	1.22	0.78	0.30	1.08	1.56	0.29	Gustatory receptor 36b	
GT_09_P064131	0.67	1.41	0.27	1.64	0.96	0.49	Gustatory receptor 97a	
GT_09_P064136	0.87	2.70	0.26	3.38	0.88	0.32	Gustatory receptor 94a	
GT_09_P064261	0.74	1.90	0.24	1.30	1.24	0.24	Gustatory receptor 21a	CO_2
GT_09_P016231	0.88	2.90	0.24	2.86	0.88	0.15	Gustatory receptor Gr9a	
GT_09_P064141	0.71	2.66	0.23	3.17	0.67	0.11	Gustatory receptor 93a	
GT_09_P064181	0.85	2.32	0.22	2.37	1.21	0.43	Gustatory receptor 58b	
GT_09_P056851	0.96	1.29	0.21	2.01	0.46	0.09	Gustatory receptor 93b	
GT_09_P064196	1.00	1.86	0.19	2.42	1.01	0.59	Gustatory receptor 47b	
GT_09_P064176	0.86	1.80	0.19	2.00	1.02	0.17	Gustatory receptor 58c	
GT_09_P064156	0.91	1.75	0.18	2.38	0.67	0.45	Gustatory receptor 59e	
GT_09_P079951	0.96	0.63	0.17	1.71	0.87	0.73	Gustatory receptor 2a	
GT_09_P056866	0.68	1.82	0.16	2.12	0.81	0.42	Gustatory receptor 77a	
GT_09_P056846	0.82	1.76	0.15	1.73	0.81	1.40	Gustatory receptor 93c	
GT_09_P056896	0.87	2.59	0.15	2.58	0.77	0.14	Gustatory receptor 36c	
GT_09_P064146	0.90	2.39	0.13	3.57	0.72	0.13	Gustatory receptor 68a	
GT_09_P022236	0.99	2.37	0.13	1.76	0.77	0.59	Gustatory receptor 33a	
GT_09_P057221	0.91	1.51	0.13	1.91	0.75	0.13	Gustatory receptor 98d	
GT_09_P056876	0.91	2.88	0.13	3.99	0.63	0.12	Gustatory receptor 64b	
GT_09_P057226	0.79	2.00	0.12	2.22	0.65	0.67	Gustatory receptor 98c	
GT_09_P057231	0.98	2.22	0.12	5.05	0.64	0.24	Gustatory receptor 98b	
GT_09_P056946	0.68	1.50	0.12	2.22	0.62	0.14	Gustatory receptor 22b	

Table 5 continued

Agilent code	Control	Nano-SiO2	Nano-Al-SiO2	Nano-Au	Nano-Ag	Nano-ZnO	Protein name	Ligands
GT_09_P056856	0.72	2.29	0.11	2.86	0.58	0.09	Gustatory receptor 92a	
GT_09_P056936	0.71	2.29	0.10	2.73	0.51	0.18	Gustatory receptor 22e	
GT_09_P056881	0.74	1.82	0.09	1.89	0.44	0.36	Gustatory receptor 64a	
GT_09_P024846	0.85	1.91	0.06	3.03	0.33	0.12	Gustatory receptor Gr43b	
GT_09_P029176	0.81	0.67	0.05	0.85	0.09	0.35	Gustatory receptor 63a	CO_2

Column 1: Agilent code: Agilent code for gene name; Column 2: Control: Flies were not fed with any nanoparticles; Flies fed with Column 3: Nano-silica; Column 4: Nano-alumino-silicate; Column 5: Nano-Au; Column 6: Nano-Ag; Column 7: Nano-ZnO; Column 8: Name of the gustatory receptor (Gr) protein; and Column 9: Known gustatory ligands of the Grs

In order to assess biosafety, we have conducted microarray studies in the fruit fly model. The effects of nano-silica, nano-alumino-silicate, nano-gold, nano-ZnO vis a vis BSA-capped nano-Ag were compared at the genome wide level. Here, we show the effects of the nanoparticles on 63 taste/gustatory (Gr) receptors of *Drosophila melanogaster* (Table 5). Till now, the ligands of a handful of Gr-s are known. Results indicate that the effects of BSA-capped nano-Ag as a drug on the fly genome is random and therefore could be considered safe. Long-term animal studies are in progress.

To the best of our knowledge, this is the first successful clinical demonstration of fighting *M. tuberculosis* including *mdr* strains with the help of surface-modified nanosilver. We hope this approach might usher a novel strategy for fighting lethal TB in the near future. Further research on the development of different intelligently surface-modified nanosilver as well as core–shell nano-silver which might reduce bio-toxicity to a very low level is currently underway. It has not escaped our attention that use of human serum albumin would be a better choice while developing drug formulations later.

Acknowledgments This study was supported by Indian Statistical Institute (ISI) intramural grant on nanoscience for 2008-2011, NAIP-ICAR-World Bank mega-project grant no. NAIP/Comp-4/C3004/2008-2009 (PI: A. G.). D. S. was supported by DBT nanoscience infrastructure mega grant no. BT/PR9050/NNT/28/21/2007 (PI: A. G.) and DBT exploratory grant on Nanocomposites no. BT/PR8931/NNT/28/07/2007(PI,ISI:A.G.). This article has been critically examined by Mrs. Indrani Roy.

References

1. Goswami A, Singh S, Redkar VD, Sharma S (1997) Characterization of P0, a ribosomal phosphoprotein of *Plasmodium falciparum* antibody against amino-terminal domain inhibits parasite growth. J Biol Chem 272(18):12138–12143
2. Sharma S, Goswami A, Singh NJ, Kabilan L, Deodhar SS (1996) Immunogenicity of the nonrepetitive regions of the circumsporozoite protein of *Plasmodium knowlesi*. Am J Trop Med Hyg 55(6):635–641
3. Goswami A, Chatterjee S, Sharma S (1996) Cloning of a ribosomal phosphoprotein P0 gene homologue from *Plasmodium falciparum*. Mol Biochem Parasitol (Elsevier) 82(1):117–120
4. Singh S, Sehgal A, Goswami A, Waghmare S, Chakrabarty T, Sharma S (2002) Surface expression of the conserved ribosomal protein P0 on parasite and other cells. Mol Biochem Parasitol (Elsevier) 119(1):121–124
5. Rahman A, Seth D, Mukhopadhyaya SK, Brahmachary RL, Ulrichs C, Goswami A (2009) Surface functionalized amorphous nanosilica and microsilica with nanopores as promising tools in biomedicine. Naturwissenschaften 96:31–38
6. Goswami A, Rahman A, Biswas N, Ulrichs C, Büttner C, Bramhachary RL, Datta A (2009) Nanoparticle–virus complex shows enhanced immunological effect against baculovirus. J Nanosci Nanotechnol 9:1–5
7. Ulrichs C, Welke B, Mucha-Pelzer T, Goswami A, Mewis I (2008) Effect of solid particulate matter deposits on vegetation: a review. Function Plant Sci Biotechnol 2(1):56–62
8. Elechiguerra JL, Burt JL, Morones JR, Bragado AC, Gao X, Lara HH, Yacaman MJ (2005) Interaction of silver nanoparticles with HIV-1. J Nanobiotechnol 3:6
9. Kim JS (2007) Reduction of Silver Nitrate in Ethanol by Poly(N-vinylpyrrolidone). J Ind Eng Chem 13(4):566–570
10. Kubica GP, Dye WE, Cohn ML, Middlebrook G (1963) Sputum digestion and decontamination with N-acetyl L- cysteine sodium hydroxide for culture of bacteria. Am Rev Respir Dis 87:775–779
11. Forbes BA, Sahm DF, Weissfeld AS (eds) (2004) Baily & Scott's diagnostic microbiology, 2nd edn. Mosby Elsevier, St louis, MO, pp 488–506
12. World Health Organisation (2003) Treatment of tuberculosis: guidelines for national programmes, 3rd edn. World Health Organisation Geneva, Switzerland
13. Wan B, Rayner A, Harris G (2006) *Mycobacterium*. In: College JG, Fraser AG, Marmion BP, Simmons A (eds) Mackie & Mc Cartney's practical medical microbiology, 14th edn. Churchill Livingstone, London, UK, pp 332–335
14. Sritharan V, Barker RH (1991) A simple method for diagnosis of *M. tuberculosis* infection in clinical samples using PCR. Mol Cell Probes 5:585–595
15. Bandopadhyay D, Gupta S, Banerjee S, Ray D, Bhattacharya S, Bhattacharya B (2008) Adenosine deaminase estimation and multiplex polymerase chain reaction in diagnosis of extra-pulmonary tuberculosis. Int J Tuberc Lung Dis 12(10):1203–1208
16. World Health Organization. Global Tuberculosis Control, Surveillance, Planning, Financing. WHO/CDS/Tuberculosis/2002.295
17. World Health Organization. Global Tuberculosis Control, Surveillance, Planning, Financing. WHO/HTM/Tuberculosis/2005.349.Geneva, Switzerland: WHO, 2005

18. World Health Organization. Prevalence and incidence of Tuberculosis in India: A comprehensive Review, 1997. World Health Organization. Global Tuberculosis Control, Surveillance, Planning, Financing. WHO/CDS/Tuberculosis/2002.295,1998
19. Barnes P, Blotch AB, Davidson BT, Snyder DE Jr (1991) Tuberculosis in patients with immunodeficiency virus infection. N Eng J Med 324:1644–1650
20. Dooley SW, Jarvis WR, Martone WJ, Snyder DE (1992) Multidrug resistant tuberculosis (editorial). Ann Intern Med 117:191–196
21. Raviglione MC, O'Brien RJ (1998) Tuberculosis. In: Fauci AS, Braunwald E, Isselbacher KJ, Wilson JD, Martin JB, Kasper DL (eds) Harrison's principles of internal medicine, 14th edn. Mc Graw Hill Companies, Inc, Columbus, USA, pp 1010–1016
22. Chen X, Schluesener HJ (2008) Nanosilver: a nanoproduct in medical application. Toxicol Lett 176(1):1–12
23. Furno F, Morley KS, Wong B, Sharp BL, Arnold PL, Howdle SM, Baystonl R, Brown PD, Winship PD, Reid HJ (2004) Silver nanoparticles and polymeric medical devices: a new approach to prevention of infection? Nanomedicine: Nanotechnol Biol Med 3(1):95–101
24. Shrivastava S, Bera T, Roy A, Singh G, Ramachandrarao P, Dash D (2007) Characterization of enhanced antibacterial effects of novel silver nanoparticles. Nanotechnology 18:9–16 225103